CODEN [USA]: IAJPBB ISSN : 2349-7750

INDO AMERICAN JOURNAL OF
PHARMACEUTICAL SCIENCES
SJIF Impact Factor: 7.187

Available online at: http://www.iajps.com *Research Article*

# DEVELOPMENT AND CHARACTERIZATION OF LECITHIN-BASED NANOFORMULATION FOR ENHANCED DELIVERY OF ISONIAZID IN THE TREATMENT OF TUBERCULOSIS

**Ezegbe Chekwube Andrew[1], Mbah Chukwuemeka Christian[1], Ezegbe Amarachi Grace[2], Ofoefule Ifeanyi Sabinus[1]**

[1]Department of Pharmaceutical Technology and Industrial Pharmacy, University of Nigeria, Nsukka, Enugu State, 410001 Nigeria.

[2]Department of Home Science and Management, University of Nigeria, Nsukka, Enugu State, 410001, Nigeria.

**Article Received:** November 2021 **Accepted:** November 2021 **Published:** December 2021

**Abstract:**

***Background:*** *Isoniazid (INH) is a synthetic antimicrobial agent used in the treatment of tuberculosis. It is rapidly and completely absorbed after oral administration. With the advent of nanoscience and nanotechnology, nanoparticles are able to encapsulate drugs, thus protecting them against the effect of chemical and enzymatic degradation.* ***Objectives****: To develop a low dose lecithin-based nano-formulation of isoniazid, to characterize some physiochemical properties of the isoniazid nanocapsules, to evaluate the antimycobacterial activities of the isoniazid nanoparticles against Mycobacterium isolates.* ***Methods:*** *INH nanocapsules were formulated by mechanical dispersion method. Preformulation studies were done using Fourier Transform Infra-red (FTIR) spectroscopy, DSC and Design Expert® version 13, Stat-Ease Inc; Minneapolis). The final products were made into tablets and enteric coated capsules using entrisic (Capsugel®). The nanoformulations were characterized for particle size using zeta sizer, morphology by scanning electron microscopy (SEM), thermal properties by Differential Scanning Calorimetry (DSC), entrapment efficiency (EE) and in vitro release. The in vitro anti-mycobacterium activities of the nanoformulations were assessed by the method of Pires et al., (2014) comparatively with commercial brands of INH tablets.* ***Result****: The isoniazid nanocapsules had a polydispersity index range from 0.294 ± 0.04 to 0.295 ± 0.04, while the particle size ranged from 106.0 ± 0.05 to 106.1 ± 0.05 nm. The encapsulation efficiency ranged from 95.4 ± 0.37 to 95.7 ± 0.10 %. The percentage drug content ranged from 93.5 ± 0.94 to 96.4 ± 0.29 %. The weight uniformity ranged from 0.25 ± 0.04 to 0.26 ± 0.04 g, while the disintegration time ranged from 12.3 ± 0.01 to 13.2 ± 0.01 min. The in vitro release studies showed that at 8 h, 80.5 % of drug was released in batch IRL, while 99.2 % of drug was released in batch IEL. The results of the antimycobacterial studies indicated that the MICs of the INH nanocapsule formulations (IEL and IRL), were 0.03 and 0.03 µg/ml against M. smegmatis and M. bovis, respectively, which were significantly ($p < 0.05$) lower than that of the conventional tablet (0.1 µg/ml).* ***Conclusion:*** *Chitosan-fortified lecithin-based nanocapsules containing INH were formulated using locally-extracted lecithin. The nanoformulations could be further developed for application in the treatment of MDR-TB.*

***Keywords****: Isoniazid, Tuberculosis, Nanoparticles, Antimycobacterium studies, Nanotechnology.*

**Corresponding author:**

**Ezegbe Chekwube Andrew,**

*Department of Pharmaceutical Technology and Industrial Pharmacy, University of Nigeria, Nsukka, Enugu State, 410001 Nigeria.*

*Email: ezegbe.chekwube@unn.edu.ng*

QR code

*Please cite this article in press Ezegbe Chekwube Andrew et al,* ***Development And Characterization Of Lecithin-Based Nanoformulation For Enhanced Delivery Of Isoniazid In The Treatment Of Tuberculosis.,*** *Indo Am. J. P. Sci, 2021; 08(12).*

## INTRODUCTION:

Tuberculosis (TB) is a well-known infectious disease caused by the bacterium, *Mycobacterium tuberculosis* [1]. It is known to be associated with a chronic cough, night sweats, weight loss and blood-containing sputum [2]. It spreads via the air especially when people that have active TB in their lungs cough, spit or sneeze [3]. HIV/AIDS patients and active smokers usually have the presence of active infection [4]. The active form of TB is diagnosed on the basis of chest x-rays and microscopic examination of culture of body fluids. The first line drugs that are effective in the treatment of tuberculosis include isoniazid (INH), rifampicin (RIF), pyrazinamide (PZA), ethambutol (EMB) and streptomycin (SM) [5]. The resistance of the organism has been associated with the first line therapy [5]. The mycobacterial pathogens associated with tuberculosis include the *M. tuberculosis, M. bovis, M. africanum, M. microti, M. pinnipedii, M. Smegmatis* [6]. Lipid based drug delivery system has been used to provide site specific and controlled delivery of drugs that have different molecular weights [7; 8]. Lipid based formulations can be modified in order to meet wide range of product stability, toxicity and efficacy. World health organization (WHO) has recommended the use of first line drugs in the treatment of tuberculosis. The most effective treatment regimen composed of a multi-drug regimen of INH, PZA and RIF. Intensive therapy is initiated within the first two months using PZA and RIF in addition to EMB [9, 10]. Multi-drug resistant TB (MDR-TB) usually occur as a result of mismanagement of first line drugs. Although extended programs are usually recommended to achieve therapeutic effectiveness [11], the drawbacks of the regimen are associated with low patient compliance and obedience to dosage regimen. Polymeric nanoparticles are used to improve drug solubilization, stability and specific targeting, [12-14] and possibility of loading both hydrophilic and hydrophobic drugs. In the formulation of nano-capsules, the drug is solubilized in either aqueous or oily solvents and is enclosed within a polymeric membrane. INH has a wide microbiological spectrum against species of Mycobacterium such as *M. tuberculosis, M. bovis, M. kansaii* [15]. Due to its low minimal inhibitory concentration (MIC) of 0.1 to 0.7 µm against *M. tubercuosis*, it remains one of the first line drugs used in the treatment of tuberculosis [16]. Although it is frequently co-administered with other anti-tubercular drugs, it has also been used as a prophylactic agent [17]. The increase in the occurrence of MDR-TB with its deadly association with HIV necessitates the use of Nano technological approach such as encapsulation of first line drugs in lower doses than the existing forms for effective delivery. At such low but effective doses, adverse effects and cost will be reduced. The nanoparticles will protect the drug from premature degradation; improve interaction with biological barriers/environment, thereby enhancing the drug absorption and intracellular penetration. Development of low dose nanoparticles will offer safety, low cost and improved efficacy against MDR-TB. The objectives of this work include to develop a low dose lecithin-based nano–formulation of INH, to characterize some physiochemical properties of isoniazid nanoformulations, to evaluate the antimycobacterial activities of isoniazid nanoformulations against *Mycobacterium* isolates.

## MATERIALS AND METHODS:

Soybean was obtained from Nsukka main market, Enugu State, Nigeria. Pure samples of isoniazid was obtained from May and Baker, Nigeria. Hexane, acetone, ethanol, sodium chloride (MPB England), hydrogen peroxide, distilled water (STC, UNN) and chloroform (Sigma-Aldrich), Lipoid S 75® ( reference lecithin) was obtained from Lipoid GMBH, Ludwigshafan. Neusilin® (Fuji chemical industry, CO Ltd., Japan), Labrasol® (Gattefosse, Saint-Priest Cedex, France). All other reagents and solvents used were analytical grade.

### Preformulation studies

Some of the pre-formulation studies carried out in this research included: solubility analysis, compatibility of the drugs and the excipients, and formular development.

### Formular development

Experimental design by the response surface, randomized, central composite design (CCD) using Design Expert® version 13 (Stat-Ease Inc., Minneapolis) was employed for development of the formular. Nine (9) runs were performed at stirring rates of 10,000, 15,000 and 20,000 rpm, respectively (totalling 27 runs (1 axial point + 1 center point)) were performed for a face centered CCD ($\alpha = 1$) that employed 2 independent numeric factors, namely drug-lecithin combination mass ratio ($X_1$) and chitosan concentration ($X_2$), and 1 categoric factor (stirring rate, at levels 3). Two (2) dependent factors, namely particle size ($Y_1$) and entrapment efficiency (EE) ($Y_2$) were considered as the responses for the optimal formular selection.

The polynomial regression equations in the following form were used to express the influence of the independent variables ($X_1$ and $X_2$) on the selected responses in the design:

$Y = ß_o + ß_1X_1 + ß_2X_2 + ß_3X_1X_2 + ß_4X_1^2 + ß_5X_2^2$ - - - - - - -1

where Y = response/dependent variable size or EE (%)

$ß_o$ = intercept representing the arithmetic mean of all quantitative outcomes of twenty-seven runs

$ß_1$ to $ß_5$ = Coefficients computed from the observed experimental values of Y

$X_1$ and $X_2$ = Coded levels of factors or independent variables

$X_1$ $X_2$ = Factors interaction

$X_1^2$ and $X_2^2$ = Quadratic relationship terms.

The design for optimization of the nanocapsule formulations at 10,000, 15,000 and 20,000 rpm is shown in Table 1. The estimations for the vesicle size and the EE were set at the ranges of 20 to 80 nm and 95 to 100 %, respectively.

**Table 1: Design for optimization of the nanocapsule formulations at 10,000, 15,000 and 20,000 rpm**

| Run (Batch) | Factors (independent variables) | | Responses (Dependent variables) | |
|---|---|---|---|---|
| | $X_1$ (mg) | $X_2$ (mg) | Vesicle size (nm) | EE (%) |
| 1 | 0 | 0 | 80 | 100 |
| 2 | -1 | 1 | 78 | 95 |
| 3 | -1 | 1 | 74 | 98 |
| 4 | -1 | -1 | 73 | 99 |
| 5 | 0 | -1 | 70 | 95 |
| 6 | 1 | 1 | 60 | 98 |
| 7 | 1 | 1 | 65 | 97 |
| 8 | 1 | 0 | 67 | 98 |
| 9 | 1 | 0 | 68 | 96 |
| 10 | 0 | 1 | 70 | 97 |
| 11 | -1 | 0 | 64 | 98 |
| 12 | -1 | 0 | 65 | 96 |
| 13 | -1 | 1 | 50 | 95 |
| 14 | 1 | 0 | 55 | 95 |
| 15 | -1 | 0 | 57 | 97 |
| 16 | 0 | 0 | 45 | 99 |
| 17 | 0 | 0 | 40 | 100 |
| 18 | 0 | 1 | 43 | 98 |
| 19 | -1 | -1 | 49 | 97 |
| 20 | 1 | -1 | 55 | 98 |
| 21 | 1 | 1 | 57 | 99 |
| 22 | 0 | -1 | 40 | 95 |
| 23 | 1 | -1 | 55 | 97 |
| 24 | 1 | -1 | 54 | 98 |
| 25 | 0 | 1 | 25 | 99 |
| 26 | -1 | -1 | 20 | 96 |
| 27 | 0 | -1 | 28 | 95 |

**Key:** $X_1$ = Drug-lecithin combination mass ratio, $X_2$ = Chitosan concentration
-1 = low, 0 = medium, 1 = high.

**Fourier Transform Infrared Spectroscopy (FTIR)**

Analysis of samples of the ingredients was carried out for qualitative compound identification using FTIR spectroscopy [18]. The potassium bromide (KBr) pellet of approximately 1 mm diameter of the drug or drug-excipient mixture was prepared by grinding 3-5 mg of sample with 100-150 mg of KBr in pressure compression machine. The drug-KBr/drug and excipient-KBr compact was then subjected to FTIR spectroscopy [19].

**Differential Scanning Calorimetry (DSC)**

The compatibility of INH, lecithin, chitosan, and other excipients was studied using DSC-60 calorimeter. All the samples was placed in sealed aluminum pans and scanned at heating rate of 10 $^{o}$C min $^{-1}$ over temperature range of 30-300 $^{o}$C [20; 21].

**Melting Point Determination.**
The melting point of INH was determined using melting point apparatus. The pre-sealed capillary was filled by a small amount of the drug. The capillary and thermometer was placed in a melting point apparatus (Melt indexer, MP 1200). The temperature was noted when the drug starts to melt.

**Preparation of nanoparticles of INH**
The nanoparticles of INH were prepared by the mechanical dispersion method [22]. INH, lecithin and cholesterol were mixed and dissolved in Labrasol® in a beaker. Chitosan was dispersed in 100 ml of acetic acid (0.2 %) solution in distilled water overnight. STPP was then dissolved in 10 ml of distilled water and added to the chitosan dispersion and stirred using magnetic stirrer at 100 rpm for 30 min. The chitosan/STPP solution was then added to the organic solution in drops using a syringe and stirred at 10,000 rpm for 45 mins using Ultra-turax (IKA® T25 digital, Germany). Subsequently, the precipitate formed was collected after 2-3 h by centrifugation at 4,000 rpm. The nanoparticles obtained were adsorbed by mixing with Neusilin® (Fuji Chemical Industry, Japan) to form powdered product which was compressed into tablets using a single punch tableting machine ( F3 Tablet Press, Manesty, Manchester).

**Table 2: Formular for the preparation of optimized INH nanoparticles.**

| Batch | Ingredients | | | | | | |
|---|---|---|---|---|---|---|---|
| | **Isoniazid (mg)** | **Lecithin® (g)** | **Cholesterol (mg)** | **Labrasol® (%)** | **Chitosan (%)** | **STPP (%)** | **Acetic acid in distilled water qs (ml)** |
| IEL | 100.0 | 1.0 | 0.1 | 2.0 | 0.2 | 0.1 | 100.0 |
| IRL | 100.0 | 1.0 | 0.1 | 2.0 | 0.2 | 0.1 | 100.0 |

**Key:** IEL = Formulation of INH using extracted lecithin
IRL = Formulation of INH using reference lecithin

**Determination of Surface Morphology using Scanning Electron Microscope**
Shape and surface morphology of INH nanoparticles were studied using scanning electron microscopy (SEM). For shape and surface morphology the nanoparticles were mounted on metal stubs and the stub was then coated with conductive gold with sputter coater attached to the instrument. The photographs were taken using a Jeol scanning electron microscope (JEOL-JSM-AS430, Japan) [23].

**Determination of surface Morphology using Optical Microscope**
The morphology of the nanoparticles were analyzed using an optical microscope (Hund Wettzlar, Germany) attached with motic camera (Moticam 2.0MP, CMOS China) after drying of the formulation at room temperature. Approximately, 5 mg of the nanoparticles from each batch was dispersed in distilled water and a drop of the dispersion smeared on a microscope slide using a glass rod. The smear was viewed on the microscope at X40 magnification and images of the micrograph captured using motic camera.

**Determination of moisture content**
The moisture content was determined using the Mettler Toledo moisturizer. It is a computerized machine that consists of a scale oven time and a print out screen. The moisturizer was set at 105 $^{o}$C for 30 mins. To a tarred aluminum dish in the moisturizer, weighed quantity (5 g) was placed and the machine closed to start automatically. After 30 mins, the result was read off the print out screen as it appears in percentage [24].

**Drug entrapment efficiency**
The indirect method was adopted in calculating the entrapment efficiency of the nanoparticles. 100 mg of the sample formulation (nanoparticles) was dissolved in 100 ml of phosphate buffer solution (PBS) pH 6.8 and stirred at 100 rpm. The sample was further centrifuged at 10,000 rpm for 30 mins. Subsequently, 1 ml of propan-2-ol was added to the supernatant

liquid and was shaken for 10 min. 1 ml was further removed from the supernatant liquid and diluted to 10 ml using phosphate buffer solution pH 6.8. The solution was then filtered using 0.45 um pore size and analysed spectrophotometrically at 270 nm for INH [25; 26]:

$$\text{Entrapment Efficiency} = \frac{\text{total amount of drug} - \text{free drug in supernatant}}{\text{Total amount of drug}} \times 100 \quad \text{--2}$$

**Drug Loading Capacity**

LC expresses the ratio between the entrapped active pharmaceutical ingredient (API) and the total weight of the lipids. LC was determined using the relationship [26]:

$$\text{DLC} = \frac{\text{Amount of drug in supernatant}}{\text{total amount of lipid matrix used in formulation}} \quad 3$$

**Formulation of nanocapsules**

INH nanocapsules were prepared by using enteric coated capsules (entrinsic, Capsugel®). Each empty capsule shell was weighed using the electronic weighing balance (120-5DM, S. Mettler, Germany). A total of 60 capsules each containing 100 mg of INH were prepared. The formulated nanoparticles powder was filled into the capsule shell. After filling the capsule shell, the cap was used to close the shell. The weight of the capsule and powder were determined. The weight of powder to be filled in the capsule was determined using the equation [26]:

Weight of powder to be filled in the capsule = Tapped-Bulk density x Volume of the capsule ---4

**Physico-chemical properties of the nanocapsules**

**Uniformity of weight of the nanocapsules**

Twenty (20) capsules were randomly selected from each batch. Using the analytical balance (120-5DM, S. Mettler, Germany), the 20 capsules were weighed together. The mean capsule weight was then calculated. Subsequently the capsules were weighed individually and the weights of the capsules recorded. The variations of individual capsule weights from the mean weight were determined, and the percentage deviations calculated using the equation [26].

$$\text{Percentage deviation} = \frac{\text{Deviation}}{\text{Mean weight}} \times 100 \quad \text{-----5}$$

**Drug content test for nanocapsules**

A capsule from the optimized formulation was carefully opened, and the content poured into a beaker. The powder was dissolved in 50 ml of distilled water and filtered into a beaker. 1 ml of the filtrate was measured and transferred into a 100 ml volumetric flask which was made up to 100 ml mark with distilled water. 10 ml of the resulting solution was collected and put in a clean and dry test tube. The sample was analyzed using the spectrophotometer (Spectumlab 752S, Hitachi, Japan), at 280 nm for LVF [24].

**Formulation of tablets**

INH tablets were prepared by direct compression of the formulated nanoparticles powder. A total of 60 tablets per batch, each containing 100 mg of INH were prepared. A 100.0 mg of Neusilin® adsorbent was mixed with each batch of the weighed nanoparticles. Compression was done on a single punch tableting machine (F3 Tablet Press, Manesty, Manchester) [24]. All the tablets were properly stored in a drug envelop at room temperature until used.

**Physico-chemical properties of tablets**

**Uniformity of weight test**

Twenty (20) tablets were randomly selected from each batch. Using the analytical balance (120-5DM, S.Mettler, Germany), the 20 tablets were weighed together. The mean tablet weight was then calculated. Subsequently the tablets were weighed individually and the weights of the tablets recorded. The variations of individual tablet weights from the mean weight were determined, and the percentage deviations calculated [24]:

$$\text{Percentage deviation} = \frac{\text{Deviation}}{\text{Mean weight}} \times 100 \quad \text{-----5}$$

**Hardness test**

Ten (10) tablets were randomly selected from each batch. Using the Monsanto tester, the pointer was fixed at 0 Kgf. One tablet was held and placed with the tester holder and the screw adjusted until the pressure applied cracked the tablet. The hardness of each tablet was determined and recorded [24].

**Friability test**

Ten (10) tablets were selected at random from each batch. Subsequently, they were dedusted and accurately weighed together in an analytical balance. The dedusted tablets were then placed into the friabilator which was set to rotate at 25 rpm for 4 min. Then the tablets were removed, dedusted and re-weighed. The mean loss in weight and percent friability was then calculated. The friability test was repeated 3 times. The mean and standard deviation were then calculated [24]:

$$\text{Friability test} = \frac{\text{initial weight} - \text{final weight}}{\text{initial weight}} \times 100 \quad \text{-----6}$$

**Disintegration test**

Six (6) tablets were selected at random from each batch using the Erweka disintegrating unit and distilled water as the disintegrating medium maintained at 37 ± 1.0 ºC. One tablet was placed into each tube of the disintegrating unit. The time taken for each tablet to completely break down to particles and pass through the wire mesh was recorded. The mean disintegration time and standard deviation from each batch was calculated [24].

**Drug content test**

A tablet from the optimized formulation was pulverized using mortar and pestle and the content poured into a beaker. The powder was dissolved in 50 ml of distilled water and filtered into a beaker. 1 ml of the filtrate was measured and transferred into a 100 ml volumetric flask which was made up to 100 ml mark with distilled water. 10 ml of the resulting solution was collected and put in a clean and dry test tube. The sample was analyzed using the spectrophotometer (Spectumlab 752S, Hitachi, Japan) at 270 nm for INH [24].

**Dissolution studies**

The *in vitro* drug release studies were carried out using tablet dissolution test apparatus (Erweka DT-D, Heusens-tamm, Germany) [27]. Initially, 900 ml of 0.1 N HCl at (pH 1.2) was used as the dissolution medium for 2 h at 50 rpm, maintained at 37 ± 1.0 ºC. Samples were withdrawn at 5, 15, 30, 45, 60, 120 min in 0.1 N HCl. The dissolution medium was then changed to 900 ml of PBS (pH 6.8) and samples were withdrawn at 3, 4, 6, 7, 8, h intervals. The samples were appropriately diluted with PBS (pH 6.8) and assayed spectrophotometrically at 270 nm for INH [27].

***In vitro* drug release kinetics**

Various kinetic models were used to describe the *in vitro* release kinetics and mechanisms of drug release from the nanoparticles. The zero-order kinetics explains the systems where the drug release rate is independent of its concentration (eqn. 7). The first order kinetics is used to describe the release from systems where the release rate is dependent on concentration (eqn. 8). Higuchi model describes the release of drugs from the insoluble matrix as a square root of time (eqn. 9). Korsmeyer is used to describe the drug release from a polymeric system (eqn. 10 ) [27; 28]:

$C_o - C_t = K_o t$

$C_t = C_o + K_o t$ - - - - - - - - - -7

$C_t$ is the amount of drug released at time t,

$C_o$ is the initial concentration of drug at time t = 0,

$K_o$ is the zero-order rate constant.

$\text{Log } C = \log C_o - K_1 t/2.303$ - - - - - - - - - - 8

$K_t$ is the first order rate equation expressed in time $^{-1}$ or per hour,

$C_o$ is the initial concentration of the drug, C is the percent of drug remaining at time t

$ft = Q = KH \cdot t_{1/2}$ - - - - - - - - - - 9

where, Q is the amount of drug released in time t per unit area , KH is the Higuchi dissolution constant

$Mt / M\infty = K_{kp} t^n$ - - - - - - - - - - 10

where, Mt / M∞ is a fraction of drug released at time t, $K_{kp}$ is the Korsmeyer release rate constant and n is the release exponent. The n value is used to characterize different release for cylindrical shaped matrices and the value of n characterizes the release mechanism of drug.

**Antimycobacterial activity of optimized formulations**

The antimycobacterial activity of the formulations was carried using Tetrazolium (MTT) dye assay of micro broth dilution technique [29, 30]. Each formulated tablet was dissolved in 1 ml DMSO and 9 ml sterile water (1:10 dilution) and further diluted 1:10 in 7H9 Middle brook broth to give a final concentration of the following:

1. Sample A: IEL 890 µg/ml
2. Sample B: IRL 930 µg/ml
3. Sample C: Reference INH tablet 30 µg/ml
4. Sample D: pure powder of INH 25 µg/ml (prepared by dissolving 250 mg of INH in 10 ml DMSO and dilute in 1:1000 by dispensing 30 µl of INH in 30 ml 7H9 Middlebrook broth).

One hundred microliter of each sample was transferred first row of micro well plate (96 micro titer plate). 50 µL of 7H9 Middlebrook broth supplemented with albumin dextrose complex (ADC) was transferred to 2nd row of micro well plate. 50 µL of test solution was transferred from 1st well to 2nd well, mixed thoroughly by pipetting up and down four times, and continue the process to well 11 from which 50 µL was withdrawn and discard. 50 µL of diluted culture (*Mycobacterium bovis* (BCG) and *Mycobacterium smegmatis* (*M. smeg*) was added to all wells of the micro well plate respectively and incubated at 37 $^{O}$C for 7 days. Post

incubation 20 µL of tetrazolium salt dye was added to all well and allow to incubate for 1-2 h.

**Data analysis**

All the measurements were repeated at least thrice and the data obtained analyzed by Student *t*-test and One-Way Analysis of Variance (ANOVA). Statistical analysis was performed using Statistical Product and Services Solution software (SPSS, version 22.0 Inc., Chicago IL, USA) and Excel Microsoft Office version 2012. The results were presented as mean ± SD, and statistical differences between means considered significant at ($p < 0.05$).

## RESULTS AND DISCUSSION:

**Formular development**

The actual quantities of the variables for the CCD for each batch and the responses are shown in Table 3. The responses obtained ranged from 31.1 to 128.3 nm and 36.1 to 86.0 % for the vesicle size and EE, respectively.

**Table 3: Actual quantities for the optimization of the nanocapsule formulations**

| Runs | Independent Factors | | | | Responses | |
|---|---|---|---|---|---|---|
| | Actual quantities for $X_1$ (mg) | $X_1$ | $X_2$ (mg) | Stirring rate (rpm) | Vesicle size (nm) | EE (%) |
| 1 | 200:1000 | 1:5 | 0.2 | level 3 of C | 66.9 | 79.4 |
| 2 | 200:50 | 4:1 | 0.4 | level 3 of C | 47.8 | 73.4 |
| 3 | 200:50 | 4:1 | 0.4 | level 2 of C | 31.1 | 82.2 |
| 4 | 200:50 | 4:1 | 0.1 | level 3 of C | 62.7 | 59.8 |
| 5 | 200:1000 | 1:5 | 0.1 | level 1 of C | 34.2 | 58.7 |
| 6 | 200:2000 | 1:10 | 0.4 | level 3 of C | 114.8 | 55.2 |
| 7 | 200:2000 | 1:10 | 0.4 | level 2 of C | 128.3 | 46.4 |
| 8 | 200:2000 | 1:10 | 0.2 | level 1 of C | 79.5 | 55.9 |
| 9 | 200:2000 | 1:10 | 0.2 | level 3 of C | 125.1 | 56.4 |
| 10 | 200:1000 | 1:5 | 0.4 | level 3 of C | 124.9 | 52.5 |
| 11 | 200:50 | 4:1 | 0.2 | level 2 of C | 72.1 | 67.3 |
| 12 | 200:50 | 4:1 | 0.2 | level 1 of C | 50.4 | 70.2 |
| 13 | 200:50 | 4:1 | 0.4 | level 1 of C | 78.9 | 50.5 |
| 14 | 200:2000 | 1:10 | 0.2 | level 2 of C | 35.6 | 67.4 |
| 15 | 200:50 | 4:1 | 0.2 | level 3 of C | 87.0 | 65.8 |
| 16 | 200:1000 | 1:5 | 0.2 | level 2 of C | 48.0 | 67.7 |
| 17 | 200:1000 | 1:5 | 0.2 | level 1 of C | 70.3 | 50.3 |
| 18 | 200:1000 | 1:5 | 0.4 | level 1 of C | 67.1 | 61.5 |
| 19 | 200:50 | 4:1 | 0.1 | level 1 of C | 71.7 | 48.9 |
| 20 | 200:2000 | 1:10 | 0.1 | level 2 of C | 66.9 | 68.1 |
| 21 | 200:2000 | 1:10 | 0.4 | level 1 of C | 53.4 | 36.1 |
| 22 | 200:1000 | 1:5 | 0.1 | level 3 of C | 52.3 | 55.6 |
| 23 | 200:2000 | 1:10 | 0.1 | level 3 of C | 54.4 | 74.2 |
| 24 | 200:2000 | 1:10 | 0.1 | level 1 of C | 78.4 | 81.9 |
| 25 | 200:1000 | 1:5 | 0.4 | level 2 of C | 44.9 | 43.6 |
| 26 | 200:50 | 4:1 | 0.1 | level 2 of C | 47.5 | 86.0 |
| 27 | 200:1000 | 1:5 | 0.1 | level 2 of C | 42.6 | 57.7 |

**Key:** $X_1$ = Drug-lecithin combination mass ratio (mg), $X_2$ = Chitosan concentration (mg). Stirring rates at level 1 = 10,000, level 2 = 15,000 and level 3 = 20,000 rpm.

The responses were analysed by analysis of variance (ANOVA) at 95 % confidence interval and fitted to statistical models using the Design Expert®, to obtain relevant parameters as shown in Tables 4 and 5. It was observed that the best-fitted was the quadratic model.

**Table 4: Statistical parameters obtained for the ANOVA and CCD**

| Source/parameter | Vesicle size | EE |
|---|---|---|
| Model | quadratic | quadratic |
| P-value | 0.1780 | 0.0174 |
| $R^2$ value | 0.5039 | 0.5761 |
| Adjusted $R^2$ | 0.1401 | 0.2653 |
| Predicted $R^2$ | - 0.6023 | - 0.3919 |
| Adequate precision | 4.9251 | 4.9346 |

**Table 5: Confirmation of point optimization by face-centered CCD ($X_1$ and $X_2$).**

| Analyzed dependent variable (Response) | Predicted | | | Observed | Error (%) |
|---|---|---|---|---|---|
| | Mean ± SD | 95 % PI low | 95 % PI high | Mean ± SD | |
| Vesicle size (nm) | 54.18 ± 14.67 | 17.086 | 91.2839 | 70.3 ± 0.82 | 17.4054 |
| EE (%) | 99.78 ± 1.37 | 96.307 | 103.248 | 50.3 ± 0.47 | 1.6283 |

The coded polynomial equation obtained for the vesicle size was:
$V = + 55.00 + 0.3190A + 3.25B + (-0.8148)C_1 + (-7.93)C_2 + (-3.50)AB + 1.53AC_1 + 1.34AC_2 + (-7.52)BC_1 + 4.22BC_2 + 4.62A^2 + (-3.71)B^2$ ;

while that of the entrapment efficiency was:
$EE = 99.67 + 0.1738A + 0.4053B + 0.1111C_1 + 0.0000C_2 + 0.4167AB + 0.8047AC_1 + (-0.5791)AC_2 + 0.0000BC_1 + 0.4268BC_2 + (-1.33)A^2 + (-1.42)B^2$.
**were** A = Drug-lecithin combination mass ratio, B = Chitosan concentration (mg), C = Stirring rate (rpm).
The parity plot showing the distribution of observed and predicted response values for the vesicle size is shown in Fig. 1. The plot shows the effects of the interaction of the factors on the responses.

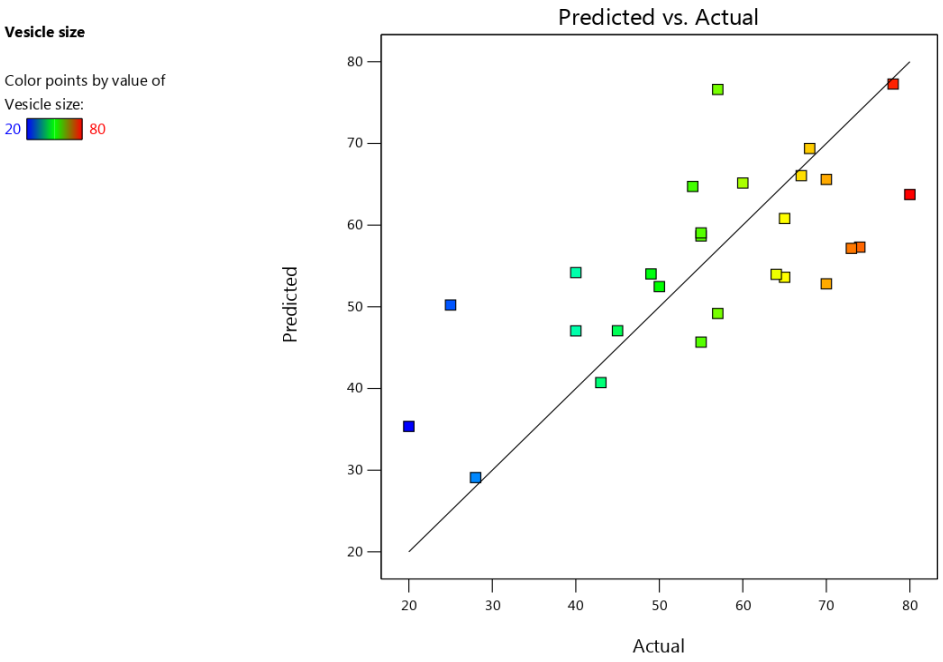


**Fig. 1**: Parity plot showing the distribution of the observed versus the predicted response values for the vesicle size

Figure 2 shows the three-dimensional response surface plots for the vesicle size. The plot shows the design space for combinations of the independent factors ($X_1$ and $X_2$ represented by A:A and B:B respectively), that would give particular vesicle size values.

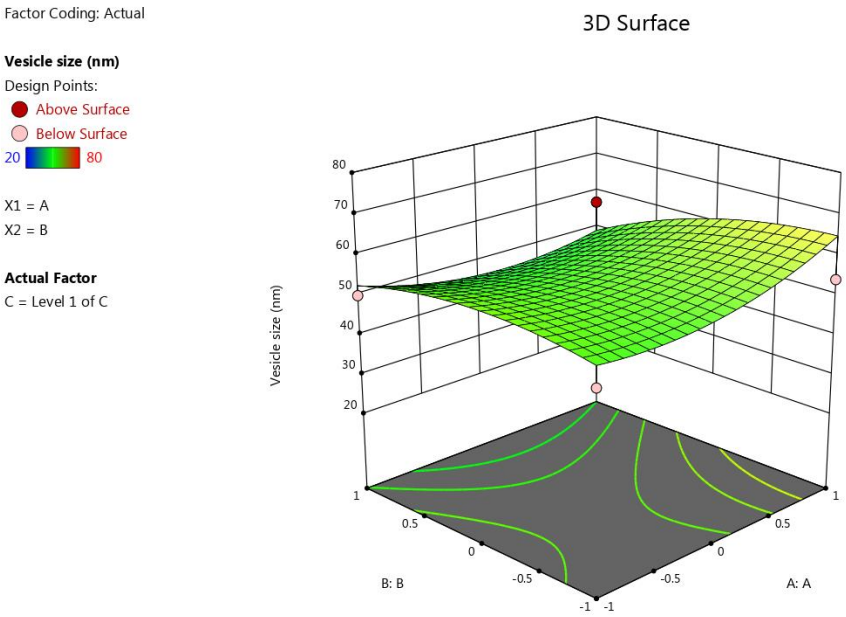


**Fig. 2**: 3D surface plots for the vesicle size.

**Confirmation location for Vesicle size.**

| A | B | C |
|---|---|---|
| 0 | 0 | Level 1 of C |

**Key**: A: 0 = Drug-lecithin ratio at medium level, B: 0 = Chitosan concentration at medium level C: 1 = Stirring rate at 10,000 rpm.

The parity plot showing the distribution of observed and predicted response values for the EE is shown in Fig. 3. The plot shows the effects of the interaction of the factors on the responses.

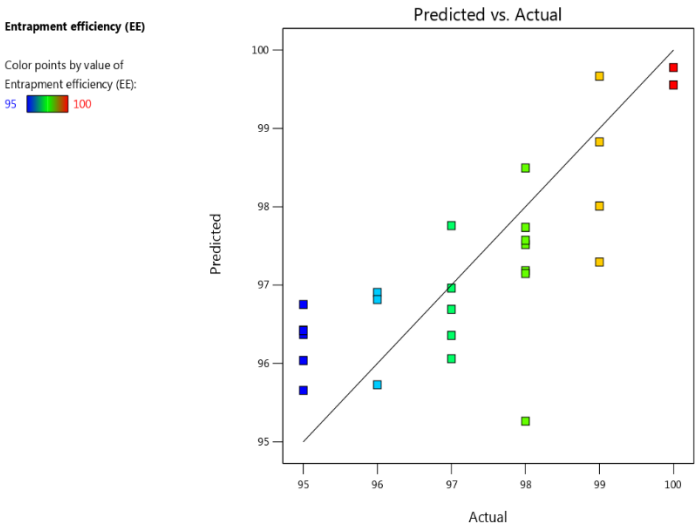


**Fig. 3**: Distribution Of Observed And Predicted Response Values

Figure 4 shows the three-dimensional response surface plots for the EE. The plot shows the design space for combinations of the independent factors ($X_1$ and $X_2$ represented by A:A and B:B respectively), that would give particular EE values.

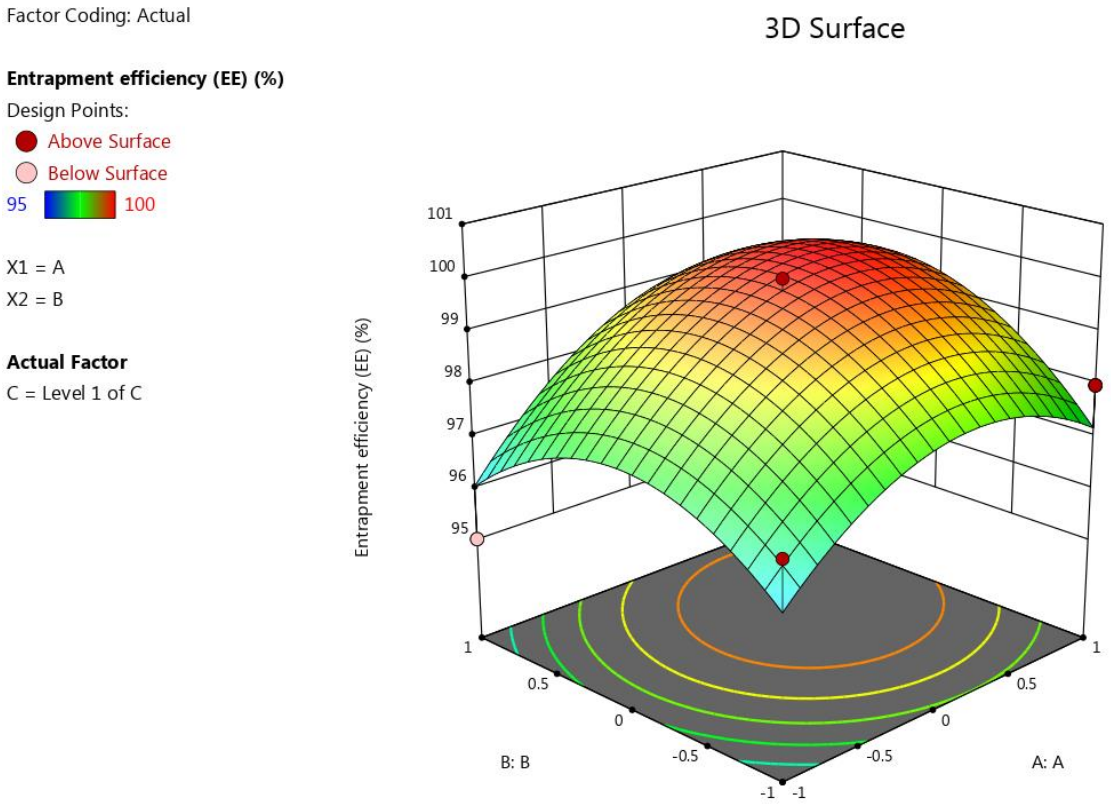


**Fig. 4**: 3D surface plots for the EE.

**Confirmation location for EE.**

| A | B | C |
|---|---|---|
| 0 | 0 | Level 1 of C |

**Key**: A: 0 = Drug-lecithin ratio at medium level, B: 0 = Chitosan concentration at medium level, C: 1 = Stirring rate at 10,000 rpm.

**FTIR Spectroscopy**

The FT-IR spectrum of batch IEL (Fig. 5) showed that the band was formed by major four characteristic peaks; situated at (3358.3 $cm^{-1}$) for OH group, (2061 $cm^{-1}$) for nitriles and carbenes , (1558 cm-1 and 1968.0) were present for C=O, C=C, C=N. The FT-IR spectrum of batch IRL (Fig. 6) showed that the band was formed by four major characteristic peaks; situated at (3354.6 $cm^{-1}$) for OH group, (2117.1 $cm^{-1}$) for nitriles and carbenes , (1558 and 1636 $cm^{-1}$) for C=O, C=C, C=N . This revealed the compatibility of the selected drug, INH. The standard band frequencies of INH showed that the major principal peaks at or around the requisite wave numbers were present thus there was no interaction between the drug and polymer [41].

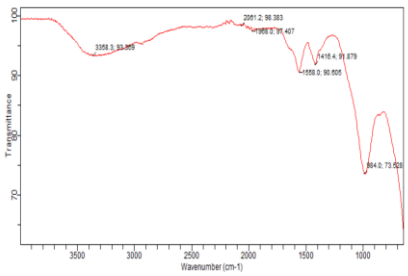

**Fig 5: FTIR result for batch IEL**

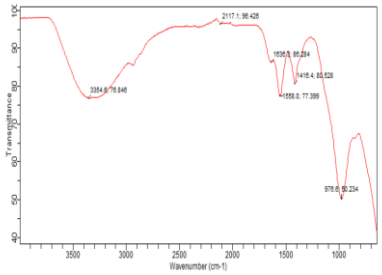

**Fig 6: FTIR result for batch IRL**

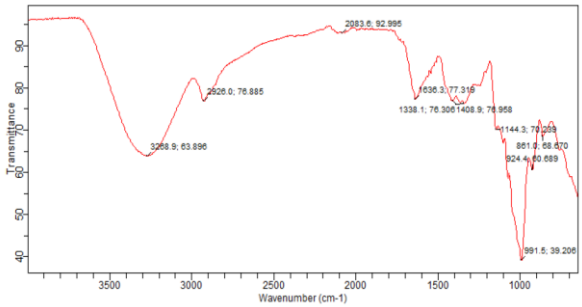


**Fig 7: FTIR of isoniazid**

**Differential scanning calorimetry (DSC)**

DSC is a thermal technique for measuring the changes that occur in a material when subjected to increased temperature (heat) at the same rate to a reference. It is employed in studying some physico-chemical properties of materials involving heat changes, including interaction of substances combined in formulations [31; 32]. Figures 8 to 10, and Tables 6 to 7 show the results of the DSC study of INH formulations.

Figure 8 shows the DSC thermograph obtained for the INH sample used in the study. An endothermic peak was observed at 121.8 ºC. However, this does not correspond to the melting point of INH, which, according to literature should be within 170 – 173 ºC [33]. This casts doubt to the purity of the drug sample used.

Figure 9 shows the thermograph obtained with the IEL formulation with a small exothermic peak at 151.2 ºC involving a – 1.61 mJ/mg energy change. This thermal transition might imply crystallization of the INH particles [34].
Similarly, the thermograph obtained for the IRL formulation (Fig. 10) presented an unclear picture with small transition peaks at 105.2 ºC and 147.3 ºC

**Table 6: Results of the DSC studies of the INH formulations.**

| Sample | Thermal change (ºC) | | | | Interpretation | Heat change (Enthalpy) (mJ/mg) |
|---|---|---|---|---|---|---|
| | Type | Onset | Endset | Mid | | |
| Isoniazid (INH) | exothermic | 76.2 | 145.4 | 121.8 | crystallization | 271.0 |
| IEL | exothermic | 89.0 | 130.1 | 114.9 | crystallization | 219.0 |
| | exothermic | 148.5 | 154.8 | 151.2 | crystallization | 1.61 |
| IRL | | 79.0 | 123.0 | 105.2 | not clear | 193 |
| | | 146.4 | 149.0 | 147.3 | not clear | 0.24 |

**Key**: IEL = Formulation of INH using extracted lecithin
IRL = Formulation of INH using reference lecithin

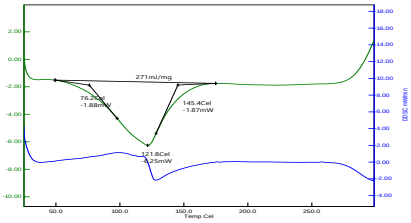

**Fig. 8: DSC thermogram of INH**.

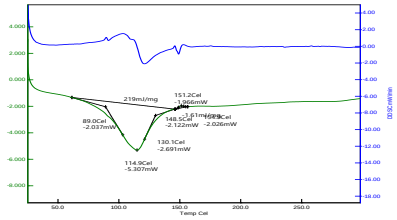

**Fig. 9: DSC thermogram of IEL**

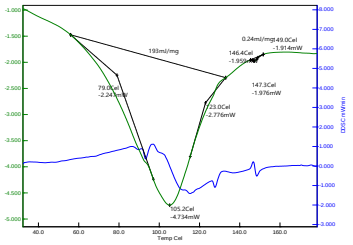

**Fig. 10: DSC thermogram of IRL.**

**Morphology using scanning electron microscope (SEM)**

Figures 11 to 14 show the detailed morphological features of the nanoparticles based on optimized parameters as obtained from the scanning electron microscope. The micrographs showed that the nanoparticles were spherically shaped, although Ramadoss and co-workers reported that the formulated nanoparticles had spherical shape with size ranging from 25 to 55 nm [33]. Overall, the INH nanoparticles were spherically shaped with a smooth surface and spherical vesicles were present.

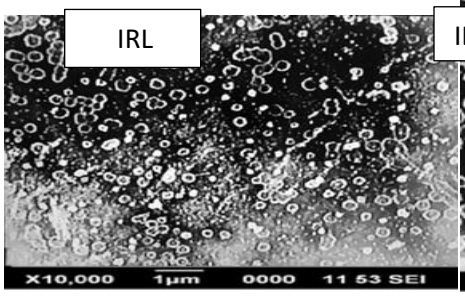


**Fig. 11.**

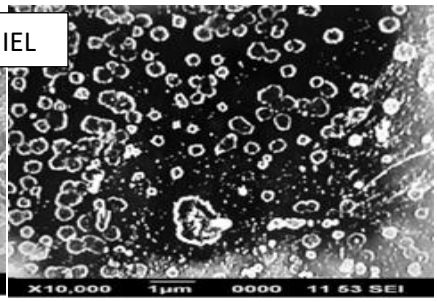


**Fig. 12**

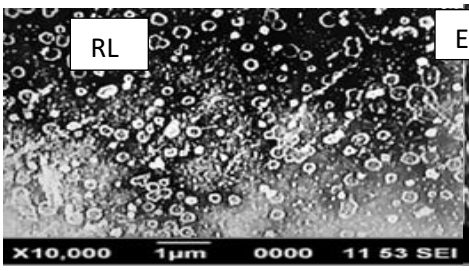


**Fig. 13.**

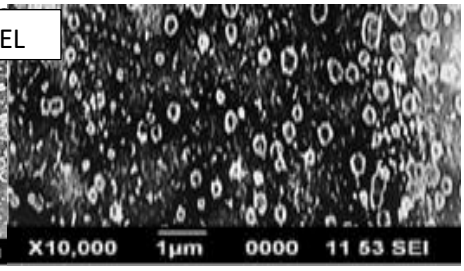


**Fig. 14.**

**Key:** Fig. 11: SEM photomicrographs of the IRL formulation, Fig. 12: SEM photomicrographs of the IEL formulation, Fig. 13: SEM photomicrographs of the RL formulation,
Fig. 14: SEM photomicrographs of the EL formulation.

**Polydispersity Index**

Table 8 shows the polydispersity index of the optimized batches. Polydispersity Index is a representation of the distribution of size population within a given sample [35]. PDI of the selected formulations is shown in Table 8. This is usually an indication of the uniformity of the particle size. From the result obtained, the isoniazid prepared with the reference lecithin had lower PDI values compared to that obtained from extracted lecithin. The overall PDI values were low and there was no significance difference ($p > 0.05$) across the sub-batches.

**Table 8: The PDI values of optimized batches**

| Batch | PDI |
|---|---|
| IEL | 0.295 ± 0.04 |
| IRL | 0.294 ± 0.04 |

**Key:** IEL: Formulation of INH using extracted lecithin
IRL: formulation of INH using reference lecithin

**Particle Size**

The particle sizes of orally administered INH significantly affect their oral absorption and bio-distribution, which ultimately determine the therapeutic efficacy. It is important to mention that although this is a nanoparticle formulation, we cannot rule out the presence of microparticles. Overall INH nanoparticles were spherically shaped with a rough surface. Particle size may be a function of either one or more of the following: formulation excipients, degree of homogenization, homogenization pressure, rate of particle size growth, crystal habit of the particle [36]. Presence of active drug in the formulation and the need to achieve thermodynamic stability in the absence of electrostatic repulsion are usually motivating factor to particle size change. All the formulations with reference lecithin showed a smaller size when compared with their extracted counterparts. Therefore, In terms of increase in particle size IEL> IRL. Additionally, the polymer concentration and the amount of lecithin added to the formulation may affect the particle size distribution [36].

**Table 9: Particle size of the optimized formulations**

| Batches | Particle size (nm) |
|---|---|
| IEL | 106.1 ± 0.05 |
| IRL | 106.0 ± 0.05 |

**Morphology using optical microscope**

Figures 15 to 18 shows the surface morphology of the optimized formulation batches that were carried out using the moticam camera. The nano-formulations had spherical shapes in different sizes, smooth surfaces and presence of vesicles. According to Ramadoss and co-workers [37]., the nanoparticles that was formulated had spherical shapes.

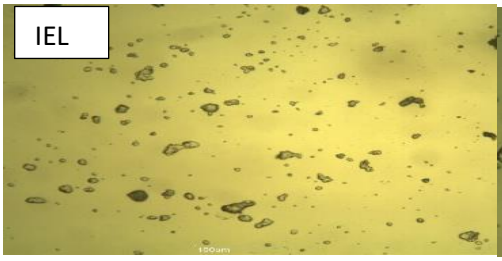


**Fig. 15**

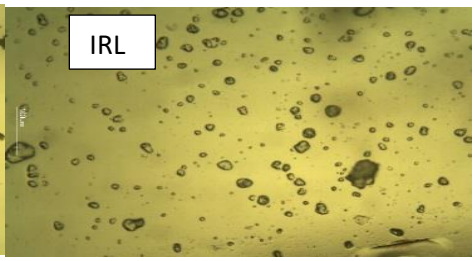


**Fig. 16**

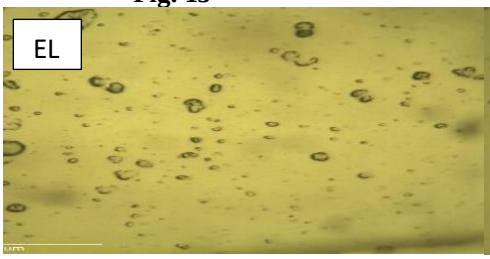


**Fig. 17**

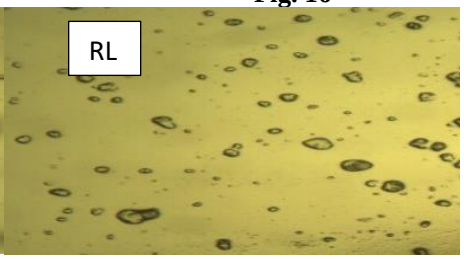


**Fig. 18**

**Key:** Fig. 15: optical photomicrographs of the IRL formulation,
Fig. 16: optical photomicrographs of the IEL formulation,
Fig. 17: optical photomicrographs of the extracted lecithin
Fig. 18: optical photomicrographs of the reference lecithin

**EE, LC, percentage yield, drug content and uniformity of weight of optimized formulations.**

The EE was determined using the indirect method [38]. This was done by determining the amount of drugs entrapped within the nanoparticles by measuring the amount of free drug in the supernatant recovered after centrifugation and washing of the nanoparticles. EE can be used to judge the suitability of any drug carrier [38]. The mechanical dispersion method and solvent evaporation technique were considered as an efficient method for preparation of the INH loaded nanoparticles, since they could avoid high temperatures. Similar results were obtained by Rojanarat and co-workers (2012), who found that as the concentration of polymer increases, the EE and drug content increased with more encapsulation of the drug particles [38]. As shown in Table 10, the EE of the optimized formulations were above 90 %. High EE is very important to reduce drug wastage.

**Table 10: Results obtained for the EE, LC, percentage yield, drug content and uniformity of weight of the optimized nanocapsule formulations.**

| Batch | EE (%) | LC (%) | Yield (%) | Drug content (%) | Uniformity of weight (mg) (n = 20) |
|---|---|---|---|---|---|
| **IEL** | 95.4 ± 0.37 | 27.7 ± 0.08 | 89.48 ± 0.41 | 96.4 ± 0.29 | 165.0 ± 0.01 |
| **IRL** | 95.7 ± 0.10 | 26.6 ± 0.07 | 91.48 ± 1.44 | 93.5 ± 0.94 | 170.0 ± 0.02 |

**Key:** IEL = Formulation of INH using extracted lecithin
IRL = Formulation of INH using reference lecithin

The result of the release study of IEL formulation is presented in Fig 19. It showed that the amount of drug released increased with time. The cumulative release behavior of the IEL nanoparticles showed that over the 8 h period, the amount of drug released was 80.3 %. According to Margret and co-workers (2012), 99.53 % of INH was released at 45 min [33]. This was due to the absence of a cross-linking agent in the formulation. Also according to Mani and co-workers, (2013), the cumulative behavior of INH showed that INH loaded poly (lactic-co-glycolic acid) PLGA nanoparticles released 37.1 % up to 74 h. The overall *in vitro* studies reported by Mani and Saha (2013), indicated that the release of INH was completed within 12-16 h [34].

The result of the release study of IRL formulation is presented in Fig. 20. At 0.5 h, 21.7 % of the drug was released, while at 3 h, 77.5 % of the drug was released. After 8 h, the maximum release was 99.2 %. The influence of the cross-linking agent on the release of drug from the formulation was attributed to the fact that the cross-linking process usually hardens the chitosan matrix and so increased the resistance to the penetration of the release medium [39].

Figure 21 represents the release profile of IEL and IRL nanocapsule formulations. At 0.5 h, 18.6 and 27.9 % of INH was released at pH 1.2, respectively. The amount of drug released in both formulations increased steadily with time over the 8 h period. The release profile was characterized by a good sustained release properties with no burst effect. Being a sustained release dosage form, it will improve patient compliance, maintain the therapeutic action of the drug, reduce the incidence and severity of systemic side effect and the total amount of drug administered over the period of drug treatment. IRL formulation had higher value of maximum drug release than IEL formulation with a significant difference ($p < 0.05$).

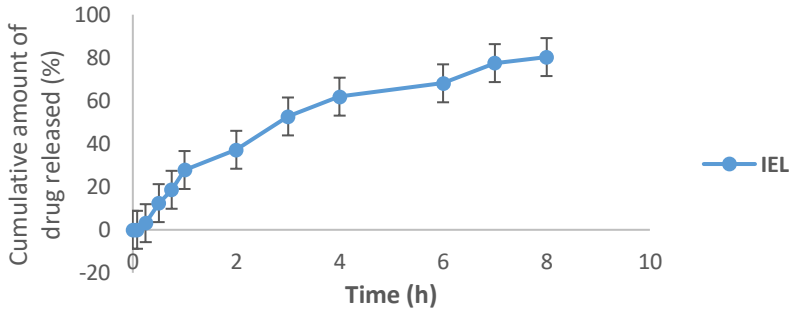


**Fig. 19: Drug release profile of IEL formulation at 0.1 N HCl (pH 1.2) and PBS (pH 6.8).**

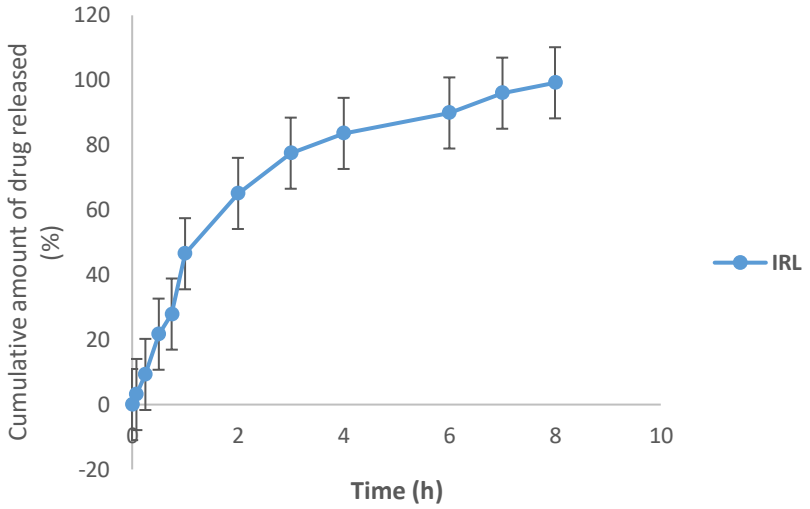


**Fig. 20: Drug release profile of IRL formulation at 0.1 N HCl (pH 1.2) and PBS (pH 6.8).**

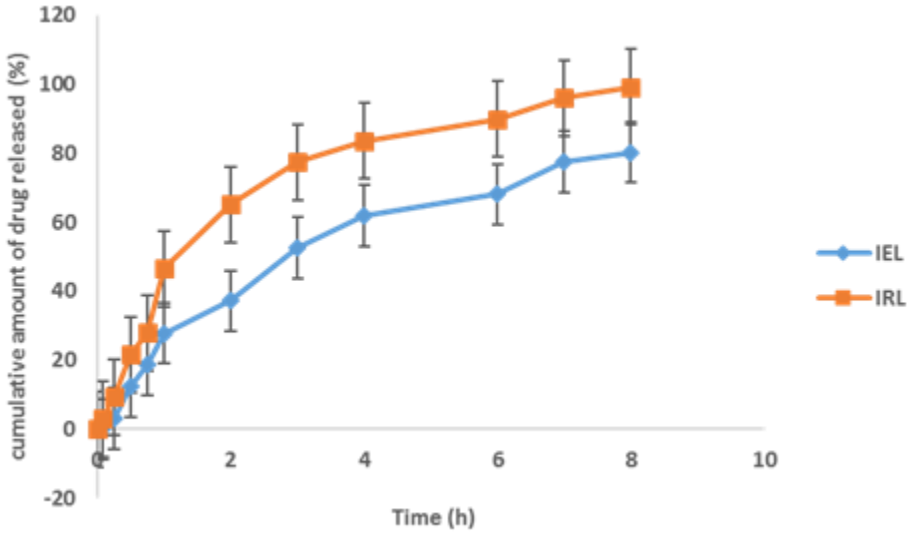


**Fig. 21: Drug release profile of the IRL and IEL formulations at 0.1 N HCl (pH 1.2) and PBS (pH 6.8).**

**Table 11: The zero, first order, Higuchi, Korsmeyer-Peppas models for drug release determination in INH formulations.**

| Batch | Zero order | First order | Higuchi | Korsmeyer-Peppas | |
|---|---|---|---|---|---|
| | $r^2$ | $r^2$ | $r^2$ | $r^2$ | n |
| **IEL** | 0.5814 | 0.9930 | 0.9247 | 0.9831 | 1.228 |
| **IRL** | 0.7743 | 0.9777 | 0.9466 | 0.9723 | 0.876 |

* $r^2$ = Coefficient of correlation, n = release exponent.

**Key:** IEL = Formulation of INH using extracted lecithin
IRL = Formulation of INH using reference lecithin.

**Table 12: Physico-chemical properties of the tablets (mean ± SD)**

| Batch | Uniformity of weight (mg) (n=20) | Hardness (N) (n=10) | Friability (%) (n =10) | Disintegration time (mins) (n=6) | Drug content (%) (n=3) |
|---|---|---|---|---|---|
| IEL | 180.5 ± 0.47 | 4.00 ± 0.07 | 0.37 ± 0.02 | 13.2 ± 0.01 | 98.4 ± 0.09 |
| IRL | 186.2 ± 0.82 | 4.23 ± 0.05 | 0.57 ± 0.17 | 12.3 ± 0.01 | 94.6 ± 0.47 |
| CI | 601.6 ± 0.47 | 5.91 ± 0.09 | 0.18 ± 0.01 | 14.8 ± 0.05 | 99.1 ± 0.08 |

**Result of the Antimycobacterium test of the optimized formulations.**

The optimized formulations were tested against two (2) clinical isolates (*M. bovis* and *M. Smegmatis*). A colour change from blue to pink indicated mycobacterial growth and the MICs was interpreted as the lowest concentration that prevented the colour change. The INH formulated with the extracted and reference lecithin (MIC = 0.03 µg/ml) exhibited promising activity [40]. Well 12 above, serves as a control for organism activity.

**Table 13 . Antituberculosis activity of different formulations against *Mycobacterium bovis (BCG).***

| Sample | MICS IN MICROWELL PLATES µg/ml against *M. bovis* (BCG) | | | | | | | | | | | | MIC values |
|---|---|---|---|---|---|---|---|---|---|---|---|---|---|
| Wells | 1 | 2 | 3 | 4 | 5 | 6 | 7 | 8 | 9 | 10 | 11 | 12 | |
| A | - | - | - | - | - | - | - | - | - | + | + | + | 0.03 |
| B | - | - | - | - | - | - | - | - | - | + | + | + | 0.03 |
| C | - | - | - | - | - | - | - | - | + | + | + | + | 0.1 |
| D | - | - | - | - | - | - | - | + | + | + | + | + | 0.06 |

**Key**: (-) = inhibition of test organism (activity), (+) = growth of test organism (no activity) Well 12 is control for organism viability, Sample A (IEL) : Formulation of INH using extracted lecithin, Sample B (IRL): Formulation of INH using reference lecithin,

Sample C: Reference isoniazid (Isoniazid,300 mg by Medico®)

Sample D: Pure powder sample of isoniazid

Table 14. **Antituberculosis activity of different formulations against *Mycobacterium smegmatis***

| Sample | MICS IN MICROWELL PLATES µg/ml against *M. smegmatis* | | | | | | | | | | | | MIC values |
|---|---|---|---|---|---|---|---|---|---|---|---|---|---|
| Wells | 1 | 2 | 3 | 4 | 5 | 6 | 7 | 8 | 9 | 10 | 11 | 12 | |
| A | - | - | - | - | - | - | - | - | - | + | + | + | 0.03 |
| B | - | - | - | - | - | - | - | - | - | + | + | + | 0.03 |
| C | - | - | - | - | - | - | - | + | + | + | + | + | 0.05 |
| D | - | - | - | - | - | - | - | - | + | + | + | + | 0.04 |

Key: (-) = inhibition of test organism (activity), (+) = growth of test organism (no activity)
Well 12 is control for organism viability, Sample A (IEL) : Formulation of isoniazid using extracted lecithin, Sample B (IRL): Formulation of isoniazid using reference lecithin. Sample C: Reference Isoniazid (Isoniazid, 300 mg by Medico), Sample D: Pure powder sample of isoniazid

## CONCLUSION:

Nanocapsules containing INH were formulated using the lecithin-samples fortified with chitosan for enhanced permeation. Although the INH nanocapsules had activities against the Mycobacterial isolates, the MICs of (LEL = 0.03 µg/ml; LRL = 0.03 µg/ml), were significantly ($p < 0.05$) higher than that of the reference commercial tablet (0.05 µg/ml).

The optimized nanoformulations showed controlled release of the active constituents over the period of 8 h, unlike the reference conventional tablet formulations. The results present the chitosan-fortified nanocapsule formulations for further exploration and development for enhanced bioavailability and application against MDR-TB.

**REFERENCES:**


1. Eker B, Ortmann J, Migliori G.B, Sotgiu G, Muetterlein R, Centis R, Hoffmann H, Kirsten D, Schaberg T, Ruesch-gerdes S and Lange C. Multidrug and extensively drug-resistant tuberculosis Germany. Emerging infectious Diseases, 2008; 14 (11), 1700-6.
2. Van Solingen D. A novel pathogenic taxon of the *Mycobacterium tuberculosis* complex. Carnetti. Characterization of an exceptional isolate. *International Journal of Systemic Bacteriology*. 1997; 47 (4), 1236-45.Eric A, Robert G, Eric D. Drug loaded nanoparticles. Preparation methods and drug targeting issues. *Eur. J. Pharm Biopharm*. 1993; 39: 73-91.
3. Hirano T, Yasuda S, Osaka Y. "The inhibitory effects of fluoroquinolones on L-carnitine transport in placental cell line". *International Journal of Pharmaceutics.* 2008; 351 (1-2), 113-8.
4. Thwaites G.E., Bhavnani S.M, Chau T.T. Randomized pharmacokinetic and pharmacodynamic comparison of fluoroquinolones for tuberculous meningitis. *Antimicrob Agents Chemother.* 2011; 55:3244–53.
5. Global tuberculosis control and World Health Organization. Available at http//www.dx.doi.org/10.1186/1472-6904-9-1. [2012].
6. Brigger I, Dubernet C, and Couvreur P. "Nanoparticles in cancer therapy and diagnosis,"*AdvancedDrugDelivery Reviews*, 2002; vol. 54, no. 5, pp. 631–651.
7. J. Panyam and V. Labhasetwar. "Biodegradable nanoparticles for drug and gene delivery to cells and tissue," *Advanced Drug Delivery Reviews*, 2003; vol. 55, no. 3, pp. 329–347.
8. Onyebujoh P, Zumla A, I. Ribeiro R. Rustomjee P. Mwaba M. Gomes, J and Grange M. Treatment of tuberculosis: present status and future prospects, Bull. *World Health Organ*. 2005; 83: 857–865.
9. WHO, Treatment of tuberculosis: guidelines for national programmes, 3rd Geneva World Health Organization, 2003.

I. Smith M. Mycobacterium tuberculosis pathogenesis and molecular determinants of virulence, *Clin. Microbiol. Rev*. 2003; 16: 463–496.

10. Park SK, Kim KD, Kim HT. Preparation of silica nanoparticles: determination of the optimal synthesis conditions for small and uniform particles. *Coll Surf*., 2002; 197:7–17.
11. Henglein A, Giersig M. Formation of colloidal silver nanoparticles: capping action of citrate. *J Phys Chem.,* 1999; 103:9533–9539
12. Qiu S, Dong J, Chen G Preparation of Cu nanoparticles from water-in-oil micro emulsions. *J Coll Interf Sci.,* 1999; 216:230–234.World *Health Organization*. . World Tuberculosis day. End TB essential. Available at
13. http://www.who.int/tb/publications. [2018].
14. World Health Organization. *Global action plan on antimicrobial resistance. Available at* http://www.who.int/iris/bitstream/10665/193736/1/9789241509763 [2015]
15. European Antibiotic Awareness Day. Available at http//ecdc.europa.eu/EAAD/Pages/home.asp. [2015]. Gierszewska M; Ostrowska C. Chitosan based membranes with different ionic crosslinking density for pharm and Indaplicatons. *Carbohyd. Polym.* 2016; 153: 501-511.
16. Qin H, Wang, Q.Q. Dong L Zhang X .Zhang Z.Y.M, Han R.Q. Reparation and characterization of magnetic Fe3O4–chitosan nanoparticles loaded with isoniazid *Journal of Magnetism and Magnetic Materials*, 2015; 381. 120–126.
17. Xiong XB, Binkhathlan Z, Molavi O and Lavasanifar A. Amphiphilic block co-polymers: Preparation and application in nano drug and gene delivery. *Acta Biomater* 2012; 8: 2017-2033.
18. Margret CR; Jayakar B; Palanisamy P. Formulation and evaluation of isoniazid and ethambutol hydrochloride combination tablet. *International Research Journal of Pharmacy*, 2012; 3 (2).
19. Guan J, Cheng P, Huang S, Wu J, Li Z and You X. Optimized preparation of levofloxacin-loaded chitosan nanoparticles by mechanical dispersion method. *Phys. Procedia*., 2011; 22:163-169.
20. Attama AA, Müller-Goymann C.C. A critical study of novel physically structured lipid matrices composed of a homolipid from *caprahircus* and theobroma oil. *Int J Pharm.*, 2006; 322(1-2): 67–78.
21. Schulze D. (1996) Measuring powder flowability: A comparison of test methods. Part I. powder and bulk engineering. CSC Publishing Inc.
22. Soppimath K S. Aminabhavi T M, Kulkaarni A R. Rudzinski. W.E. Biodegradable polymeric nanoparticles as drug delivery devices. *Journal control Rel*., 2001; 70: 1-20
23. Yaowalak B, Ampol M, Bernd WM. Chitosan drug binding by ionic interaction. Eur. *Journal Pharm. Sci*., 2006; 62:267-74.
24. British Pharmacopoeia. British Pharmacopoeia, vol. III. London. Her Majesty's Stationery Office. 6578-6585. [2009].

25. Higuchi WI, Mir NA, Desai SJ. Dissolution rate of polyphase mixtures. *Pharm Sci.*, 1965; 54: 1405-10.
26. Palomino JC, Martin A, Camacho M, Guerra H, Swings J, Portaels F. Resazurinm crotiter assay plate: Simple and inexpensive method for detection of drug resistance in *Mycobacterium tuberculosis*. *Antimicrob Agents Chemother.*, 2002; 46: 2720-2722.
27. Pires CT, Mislane AB, Regiane B, Diogenes A, Luciana D, Vera L, Rosilene F. Anti-mycobacterium tuberculosis activity and cytotoxicity of *Calophyllum brasiliense* Cambess (Clusiaceae). *Mem Inst. Oswaldo Cruz, Rio de Janeiro.*, 2014; 109 (3) : 324-329.
28. Mani G, Gopi V; Elangovan V; Rajapopalan V; Sengottuvelan B. Isoniazid loaded core shell nanoparticles derived from PLGA-PEG-PLGA tri-block copolymers. In-vitro and in-vivo drug release. *Colloids Surf B. Biointerfaces,* 2013; 104:107-15.
29. Gaurav K, Sadhnas S, Nusrat S, Gopal K, Samiv M. Optimisation, *in-vitro-in vivo* evaluation and short term tolerability of novel levofloxacin-loaded PLGA nanoparticles formulation. *Journal of Phar. Sci.* 2002; 101: 2165-2176.
30. Beny B, Nagaraja S, Korlakunta N, Abin A. Formulation and evaluation of levofloxacin nanoparticles by ionic gelation method. *Journal of Pharmacy and Pharmaceutical Sciences,* 2012; 1: 1-15.
31. Gitu Pandey, Sarita Kumari, Brahmeshwar Mistra. Preparation and characterization of isoniazid and lamivudine co-loaded polymeric microspheres, *Artificial cells, Nanomedicine and Biotechnology*, 2016; 44:8, 1867-1877.
32. Nobbmann U.I. (2014). Polydispersity- what does it mean for DLS and chromatography. Available online at: https//www.materials-talks.com/blog/2014/10/23/
33. Mumuni A. Momoh, Emmanuel C. Ossai, Omeje E. Chidozie, Omenigbo O. Precscila, Franklin C. Kenechukwu, Kenneth O. Ofokansi, Anthony A. Attama, Kunle O. Olobayo. A new lipid-based oral delivery system of erythromycin for prolong sustain release activity. *Materials Science and Engineering*, 2019; 97: 245–253.
34. Ramadoss A. B; Sathya R; Radhakrishnan R. Levofloxacin: formulation and *in-vitro evaluation* of alginate and chitosan nanospheres *Egyptian Pharmaceutical Journalm* 2015; 14:30–35
35. Rojanarat W and Nakpheng T.Levofloxacin – proliposomes-oppurtunities for use in lung tuberculosis. *Pharmaceutics,* 2012; 4:385–412.
36. Zhou SB, Deng XM, Li X . Investigation on a novel core-coated microspheres protein delivery system. *J Control Release*, 2001; 75:27-36.
37. Collins, L.A.; Franzblau, S.G. Microplate alamar blue assay versus BACTEC 460 system for high-throughput screening of compounds against *Mycobacterium tuberculosis* and *Mycobacterium avium. Antimicrob. Agents Chemother*. 1997; 41, 1004-1009.
38. Pandey R, Zahoor A, Sharma S, Khuller GK. Nanoparticle encapsulated anti-tubercular drugs as a potential oral drug delivery system against murine tuberculosis. *Tuberculosis*, 2003; 83:373–378.